

## DESIGN OF RETINAL STENT USING FINITE ELEMENT ANALYSIS

Razvan Rusovici  
Florida Institute of Technology  
Melbourne, FL, USA

Dennis Dalli  
Florida Institute of Technology  
Melbourne, FL, USA  
rrusovici@yahoo.com

Kunal Mitra  
Florida Institute of Technology  
Melbourne, FL, USA

Michael Calhoun  
Optistent Inc.  
Melbourne, FL, USA

Michael Grace  
Florida Institute of Technology  
Melbourne, FL, USA

Rudy Mazzocchi  
Optistent Inc.  
Melbourne, FL, USA

Gary Ganiban  
Eye Institute  
Melbourne, FL, USA

### ABSTRACT

The motivation for the herein presented research stems from a new retinal reattachment procedure, which consists of carefully pressing the detached retina tissue into place via a shape memory alloy (SMA) and self-expanding stent. The initial study described in this article focused on modeling the mechanical interaction among stent and neighboring human eyeball tissues: retina, choroid and sclera. The study was performed via finite element analysis (FEA). The tissues were modeled with either hyperelastic or linear elastic material models in order to predict strain distributions on retina and the rest of the eye tissues due to stent placement. The FEA model included the following eyeball tissue: retina, choroid, sclera, cornea, zonular fibres, lens, and ciliary muscle. The simulations, shown for a sample stent configuration, have shown that the strain distribution developed due to stent placement was below levels which would induce permanent retina damage at the stent location. The simulations have shown that, by assuming that the retina was subjected to physiological internal ocular pressure (16.5 mmHg) in parallel to stent pressure (2200 Pa), the retinal strain reached a maximum of 2.67% , which was below a permanent damage strain threshold of 3.3%.

### KEY WORDS

Retinal stent, finite element, shape memory alloy, retina.

### 1. Introduction

The retina is a light-sensitive tissue layer that lines the inside of the eye and relays visual information directly to the brain via the optic nerve [1]. Retinal detachment occurs when the retina is lifted or pulled from its physiological location. This condition can result in partial or total vision loss. Retinal detachment can develop in patients that suffer from mechanical impact to the eye, diabetes etc. [2-4].

Retinal detachments are generally surgically-treated. Small areas of the retina that are torn (retinal tears

and breaks), and which could lead to retinal detachment, are usually repaired using laser surgery (tissue scarring) or cryopexy (freeze treatment). Another treatment method is that involving a scleral buckle (small synthetic band), which is attached to the outside of the eyeball and pushes the wall of the eye into direct contact with the detached retina. An additional surgical method is vitrectomy. During this procedure, the surgeon would make a tiny incision in the sclera to introduce a small instrument which would remove the vitreous humour. Gas would then be injected into the eye in order to maintain the shape of the eye during the procedure and to push the retina back in contact with the wall of the eye. Once the retina would be back into the original position, either laser or cryopexy would be used to reattach the retina to the wall of the eye. While retinal detachment is successfully treated in approximately 90% of patients, many instances still exist when vision is permanently lost after the surgical procedure.

Researchers and ophthalmological surgeons from OptiStent Inc. have developed a new method and a corresponding medical device for the treatment of retinal detachment. The method was based on the placement of a shape-memory-alloy (SMA) stent inside the eyeball, which was designed to re-attach the detached retina. The SMA material chosen was NiTiNOL (Nickel-Titanium-Naval Ordnance Laboratory).

The delivery method of the initial stent device was devised to be similar to that used to deploy self-expanding cardiac stents. The stent was initially loaded within the delivery instrument. Then, the delivery instrument was placed inside the eyeball through a small incision (2-3 mm diameter) in the sclera. The stent was released and then it mechanically pressed the retina back into contact with the eyeball.

Intraocular pressure (IOP) [5] is caused by the aqueous humor, and its value is a result of continuous drainage and production of aqueous humor. The average human IOP was measured at 15-16 mm Hg. The IOP could vary throughout a 24 hours period by +/- 3.5 mmHg [1].

The implementation of the OptiStent™ retinal reattachment procedure presents many challenges. Some challenges are related to the mechanical pressure that a stent would place on the detached retina. An excessive pressure, resulting into high strains, could lead to irreversible retinal damage at the stent-retina interface. Insufficient stent pressure could defeat the procedure's purpose and potentially allow the stent to migrate within the eye cavity. Thus, a modeling approach was necessary to verify, in addition to parallel experimental efforts, whether a given stent configuration (shape, material, coiled force) would lead to strains exceeding allowable physiological values. The maximum allowable physiological retinal strain values were inferred from literature surveys and could be correlated with IOP. The maximum allowable retinal strain was found to be 3.3% or 0.033 mm/mm strain (Chen et al, 2009) [4]. This value was found to correspond to permanent retinal damage in porcine eyes, which were found to be anatomically similar to human ones. The scope and contribution of the current research is to present one procedure aimed at determining stress-strain distribution in the retina after stent implantation.

Previous finite element modeling of eye was performed in order to extract strain information in eye tissue due to physiological or non-physiological loading [6-10]. One of the greatest challenges posed to researchers was the relative incompleteness of material data [9], as well as the large variability in reported eye-tissue material properties [11-19].

## 2. Modeling

Figure 1 shows a three-dimensional computer-aided design (CAD) model of the human eye.

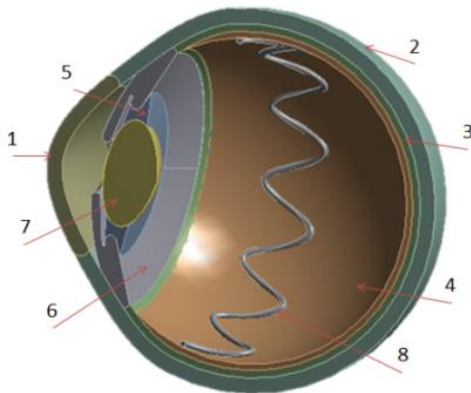


**Figure 1: Human Eyeball 3D model with SMA Stent:**  
1) Cornea, 2) Sclera, 3) Choroid, 4) Retina, 5) Zonular Fibres, 6) Ciliary Muscle, 7) Lens and 8) Nitinol Stent.

Solidworks™ modeling software was used to develop a solid eyeball, three-dimensional model. Ansys Workbench™ was used to mesh and solve for the stress/strain distribution on the interior of the eyeball due to the placed stent. The eyeball model is shown in Figure 2 and was verified against specifications found in (Rossi et

al., 2011). The CAD model featured the following tissues: retina, cornea, choroid, zonular fibres, ciliary muscle, lens and sclera.

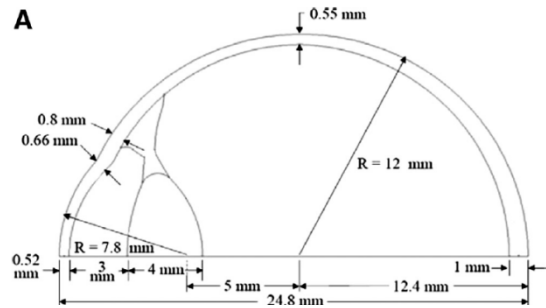


**Figure 2: Human eyeball cross-section schematics, [15].**

### 2.1 Eye Tissue Material Modeling

The procedure focused initially on material modeling within the finite element framework. Eye tissue (retina, sclera, choroid etc.) and SMA material are all non-linear. The implemented hyperelastic material models for sclera, retina and choroid (Table 3) were hyperelastic while the lens, ciliary muscles and zonular were considered to be linearly elastic. The stent was modeled using an SMA material model. The sclera and retina were modeled using Mooney-Rivlin models. The choroid was modeled using an Ogden model; the rest of the eye tissues were considered to be elastic [3, 14, 16] (Tables 1-4).

**Table 1: Material Model**

Material	Material Models
Sclera	Mooney-Rivlin 5 Paramenter
Retina	Mooney-Rivlin 2 Paramenter
Choroid	Ogden 1 <sup>st</sup> Order
Lens	Linear elastic
Ciliary muscle	Linear elastic
Zonular	Linear elastic
Stent	Isotropic nitinol

**Table 2: Retina Mooney-Rivlin Material Properties**

Material	$C_{10}$ , MPa	$C_{01}$ , MPa
Retina	0.011765	0.027

**Table 3: Choroid Ogden 1<sup>st</sup> Order Material Properties**

Material	n	$\mu$ , MPa	$\alpha$
Choroid	1	0.24	12

**Table 4: Sclera Mooney-Rivlin Hyperelastic Material Properties**

Tissue	$C_{10}$ , MPa	$C_{01}$ , MPa	$C_{11}$ , MPa	$C_{20}$ , MPa	$C_{02}$ , MPa
Sclera	54.5	-54.1	$1.05 \cdot 10^6$	$5.45 \cdot 10^5$	$5.1 \cdot 10^7$

## 2.2 SMA Modeling

SMA material models were used for stent modeling. The stresses and strains on the stent were considered to be small, thus only the elastic modulus of the SMA along the linearly-elastic portion of the stress-strain curve of the stent was adopted (Figure 3 [20]). This simplifying assumption reduced computation time while providing adequate material modeling fidelity.

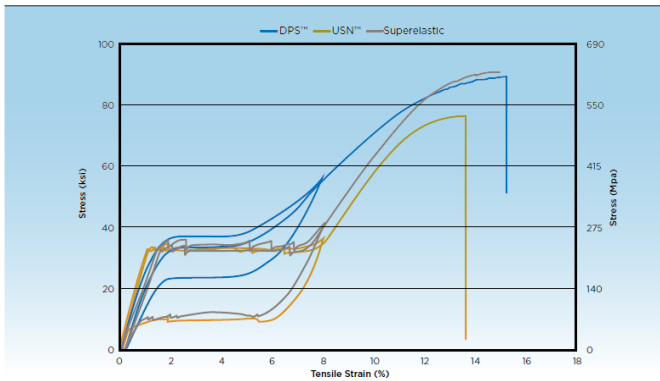


**Figure 3: Nitinol Stress-Strain Curve.**

## 3. FEA Modeling

The variable parameters pertaining to the procedure could be many and include variations in stent and eye tissue material properties, delivery temperature of the stent (stents are often compressed via cooling), geometry of the stent (shape, wire diameter, number of coils) etc. The analysis results presented herein were obtained only for a single chosen SMA stent-geometry and preloading.

The sample stent considered in the studies (Figure 4), when deployed, had a sinusoidal shape with 9 cycles per circumference. The stent also had a 0.15-mm wire diameter. The finite element model (FEM) which included stent, sclera, choroid and retina were modeled by solid finite elements (Table 5, Figure 5).



**Figure 4: Nitinol Stent, 3D CAD Design.**

**Table 5: Finite Element Mesh**

Tissue	Elements	Nodes
Sclera	11354	22228
Retina	9591	19371
Choroid	9233	18670
Lens	2989	4733
Cornea	2955	5290
Ciliary muscle	6291	11007
Zonular	2134	4210
Stent	9729	20163

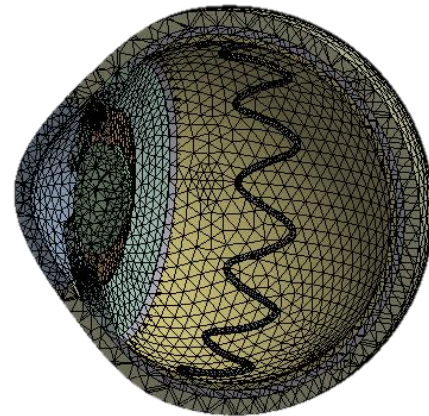


**Figure 5: Finite Element Mesh of Eyeball with Stent, Meshed via Solid Tetrahedral Finite Elements.**

The IOP was chosen to have a value of 16-mm Hg (2200 Pa) corresponding to an average human intraocular pressure (IOP) [5] with the exception of a single validation case, where IOP was 50-mm Hg. In all these numerical studies, the inserted and expanded chosen stent was modeled to also exert a 2200 Pa pressure on the eyeball.

## 4. Results

Previous studies of pig eyes [4] yielded the mechanical properties of the retina, choroid and sclera, which were used in the current research. Furthermore, a strain of 3.3%

was taken to be a permanent damage threshold for retina tissue [4].

### 4.1 Model Validation

First, the FEA model validation was performed. According to previous published research (Ethier, 2004) [1], retinal strain reached 12% when the IOP increased to 50 mmHg; 50 mmHg was found to be the threshold for catastrophic IOP. Thus, an IOP of 50-mm Hg or 6666.118 Pa was applied to the retina within the finite element model. The maximum strain results found from FEA are shown in Table 8 and Figure 6.

**Table 6: Validation Results**

Material	Literature strain at 50mmHg, %	Simulation strain at 50 mmHg, %	Difference	Percent Difference, %
Retina	12	11.108	0.892	0.743

The validation run showed good agreement with literature data [1].

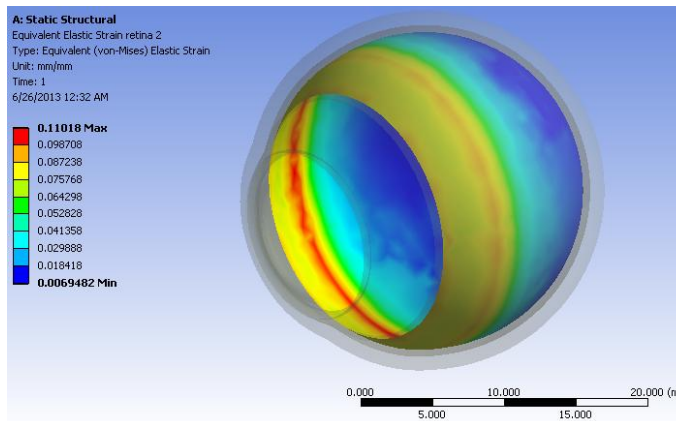


**Figure 3: Retina (von-Mises) Elastic Stress Distribution, IOP = 50 mmHg.**

### 4.2 Eye-Only FEM

This section presents the validation of the eye FEM predictions (retinal strain distribution assuming normal IOP) against published research literature.

A finite element model employing hyperelastic material models for choroid and sclera, in addition to retina was used. The IOP was set at 16-mm Hg. Resulting strain and stress distributions are shown in Figures 7 and 8, respectively.

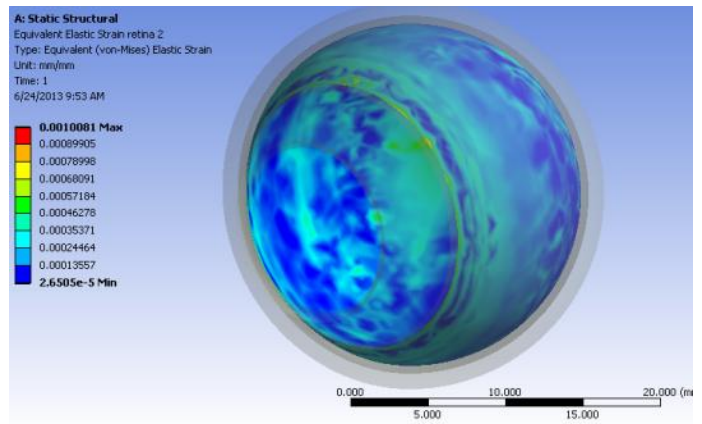


**Figure 4: Hyperelastic Retina (von-Mises) Elastic Strain Distribution.**

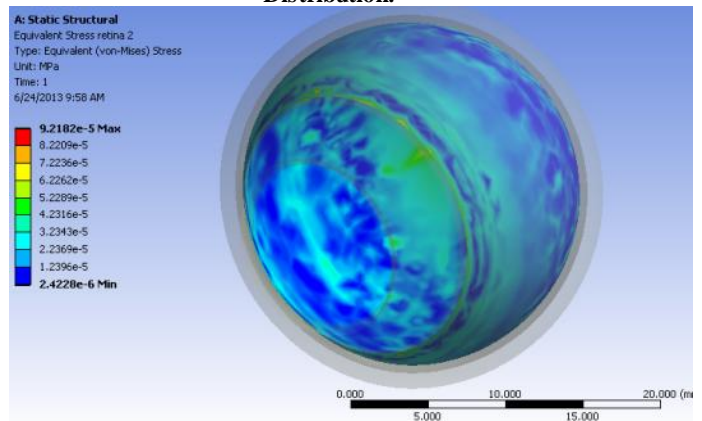


**Figure 5: Hyperelastic Retina (von-Mises) Equivalent Stress Distribution.**

It was considered useful to present the stress and strain distributions in choroid and sclera tissues as well. Figures 9 and 10 show the strain and stress distribution in the choroid layer, respectively. Figure 11 and 12 show the strain/ stress distributions in the sclera tissue, respectively.

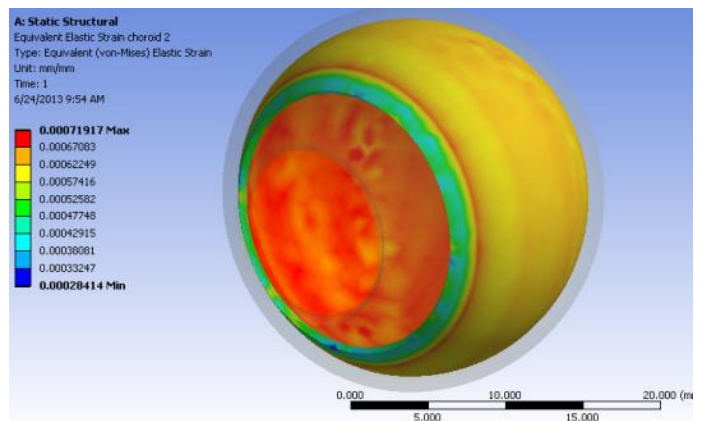


**Figure 6: Hyperelastic Choroid (von-Mises) Elastic Strain Distribution.**

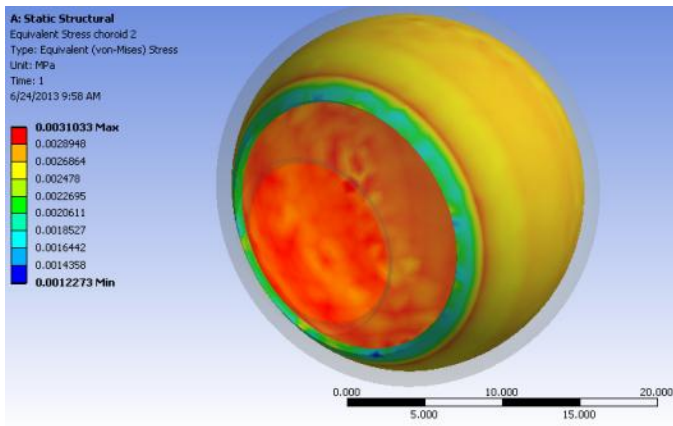


Figure 7: Hyperelastic Choroid (von-Mises) Equivalent Stress Distribution.

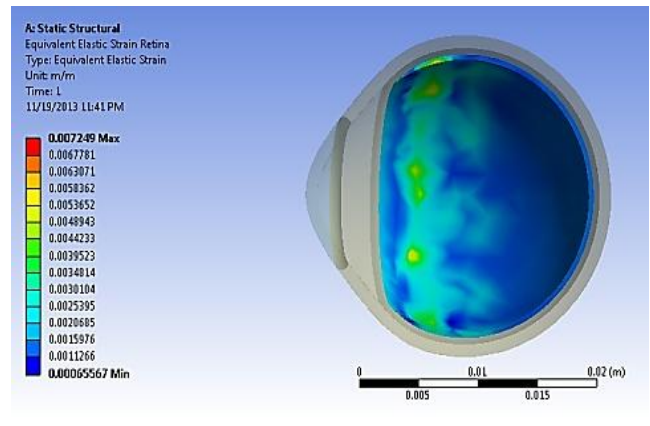


Figure 10: Retina von-Mises Equivalent Strain Distribution.

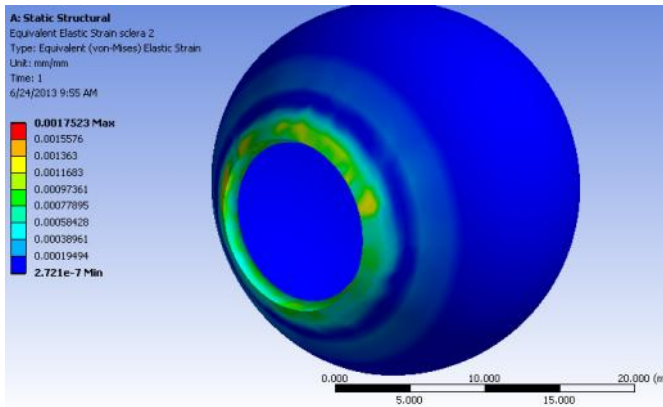


Figure 8: Hyperelastic Sclera (von-Mises) Elastic Strain Distribution.

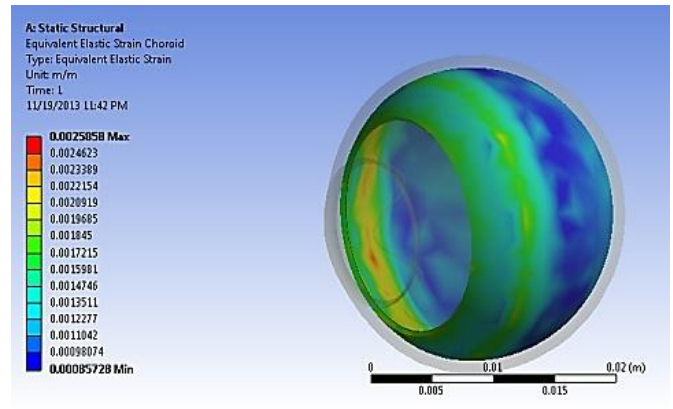


Figure 11: Choroid Von-Mises Strain Distribution.

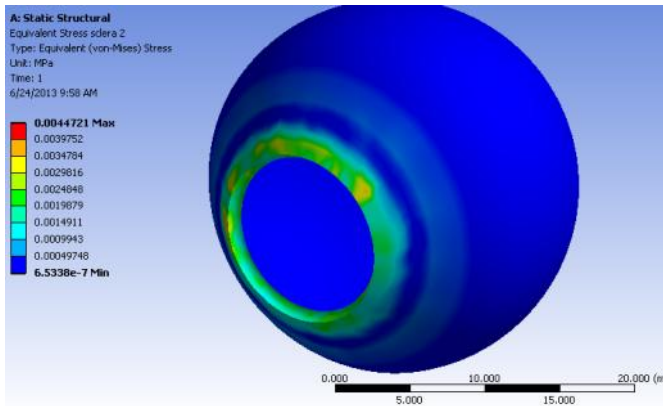


Figure 9: Hyperelastic Model Sclera (von-Mises) Equivalent Stress Distribution.

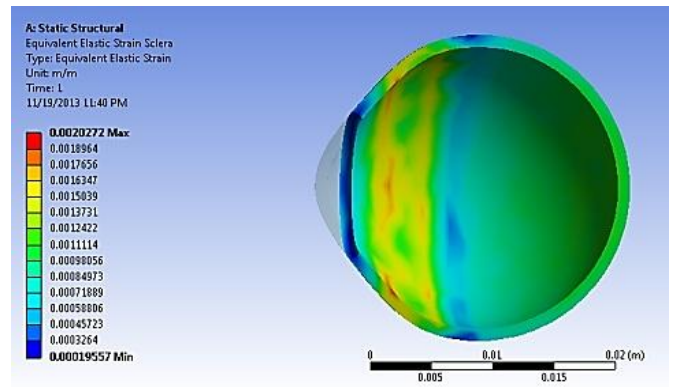


Figure 12: Sclera Von-Mises Strain Distribution.

### 4.3 Eye and Sample Stent Model

Next, an eye FEM featuring the sample stent, loaded by 16-mm Hg IOP and 2200 Pa stent pressure was analyzed. Figures 13 through 17 show the strain distribution in retina, choroid, sclera and stent, respectively.

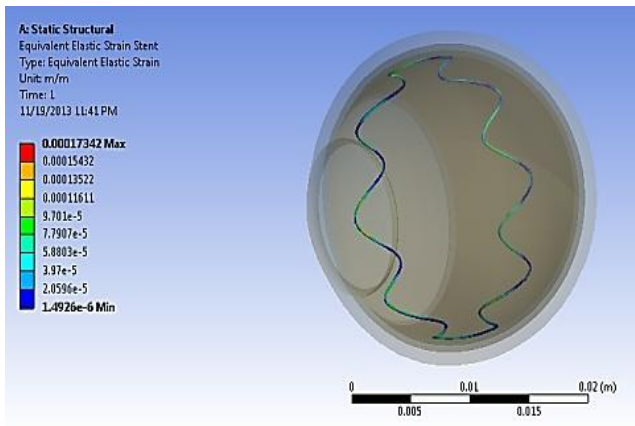


Figure 13: Stent Von-Mises Strain Distribution.

Figures 17-20 show the Von Mises stress distribution in the eye tissue and stent, respectively.

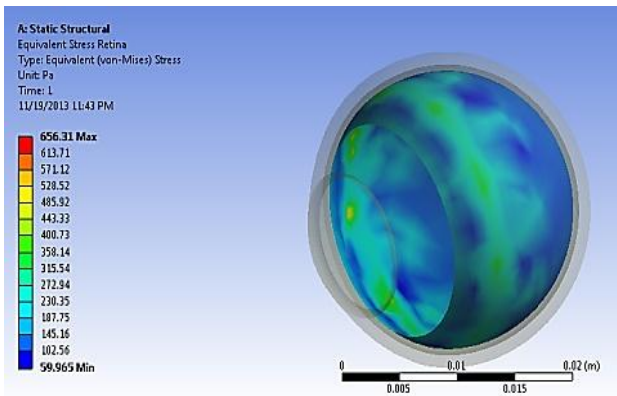


Figure 14: Retina Von-Mises Stress.

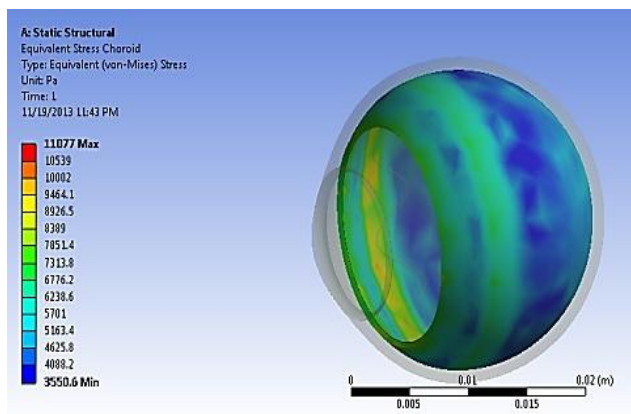


Figure 15: Choroid Von-Mises Stress.

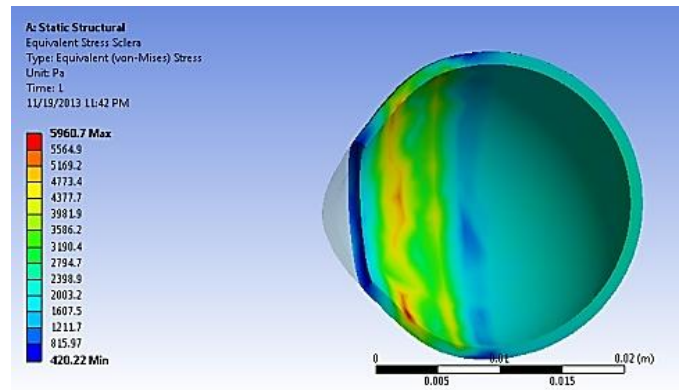


Figure 16: Sclera Von-Mises Stress.

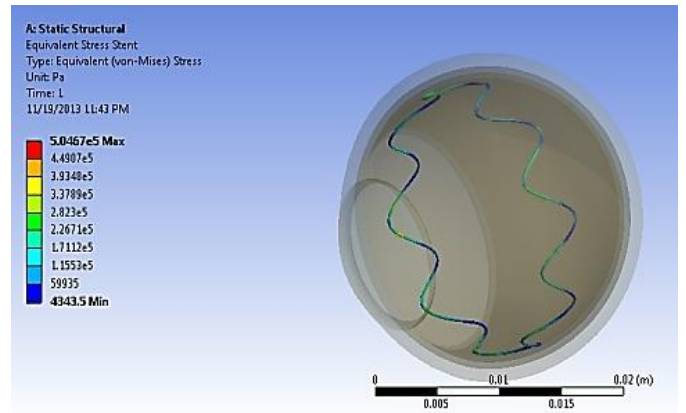


Figure 17: Stent Von-Mises Stress.

#### 4.4 Eye and 12-Loop, 0.18-Mm Diameter Stent Model

An eye FEM featuring a different stent configuration (12 loops, 0.18- mm diameter) stent, loaded by both a 16-mm Hg IOP and a 2200-Pa stent pressure was analyzed. Figures 21 through 24 show the strain distribution in retina, choroid, sclera and stent, respectively.

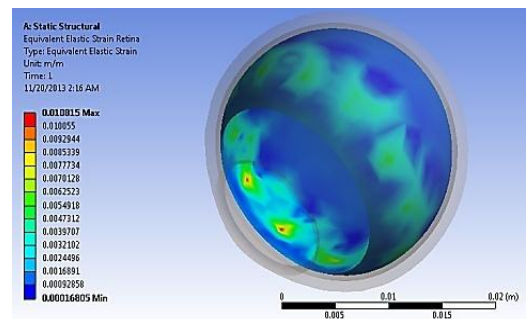


Figure 18: Retina Von-Mises Strain Distribution.

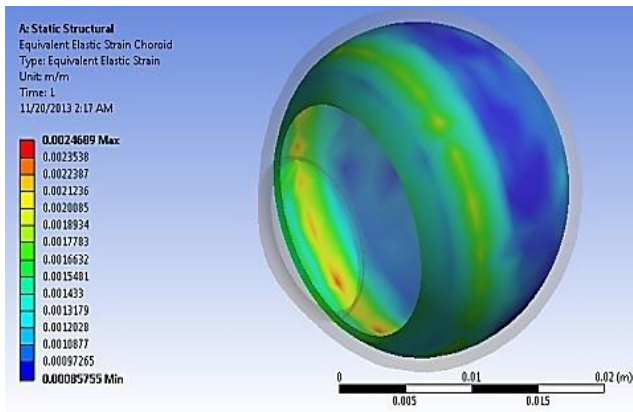


Figure 19: Choroid Von-Mises Strain.

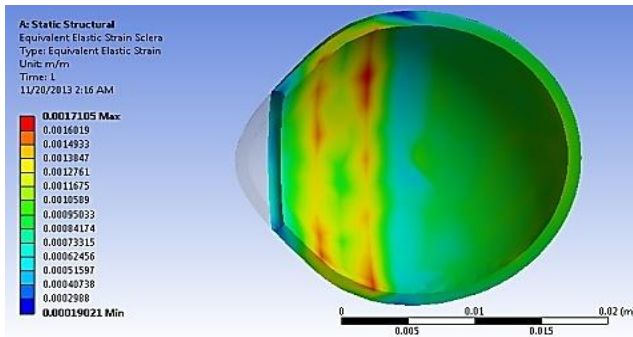


Figure 20: Sclera Von-Mises Strain Distribution.

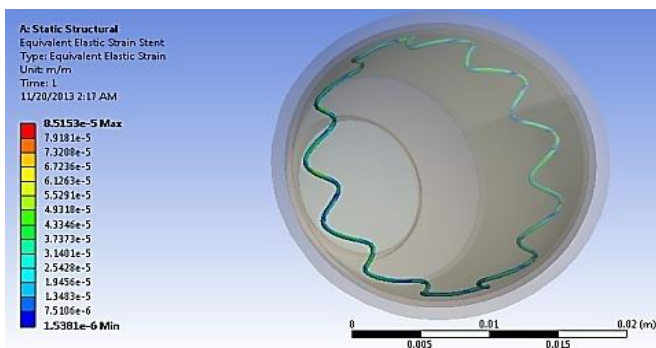


Figure 21: Stent Von-Mises Strain Distribution.

It is worth noting that with this new stent configuration, the maximum strains in retina (10%) exceeded allowable values of 3.3%!

## 5. Conclusion

The retinal repair method was initially proposed and then patented by OptiStent™, a medical device company, in collaboration with an ophthalmologic surgeon, Dr. Gary Ganiban, M.D. The contribution of the hereby presented research was to propose and validate a numerical procedure necessary for retinal stent design. The procedure, centered on FEA, would predict the strain distribution in the repaired retina due to stent placement. The stent would be designed so that its pressure on the retina would not induce irreversible damage. The FEM of

the eye and stent featured non-linear material models, anatomically-correct eye geometry and parametrically-variable stent geometry. The simple eye FEM was validated very well against published research data.

From the eye-stent FEM numerical analyses, it was evident that the incorporation of a stent produces stress concentrations at contact with the retina. The maximum von Mises retina strain was 0.1% without the sample stent vs. 0.7% with the sample stent in place. The maximum strain occurred at the contact between retina and the apex of the loops of the stent.

The stent geometry affected dramatically the strain distribution. The second stent configuration studied was found to produce levels of strain consistent with permanent retinal damage. Thus, stent design and analysis would be crucial for proper patient treatment.

As observed by others [9] there is a relative lack of complete eye-tissue material data information as well as large variation in reported values for similar material test data; this increased the challenge in defining the material models.

Future work will investigate additional stent-parameter influence on retinal strain, and further improve material models. A future parametric study will optimize stent cross-sectional profile, and number of loops per circumference. These parametric studies would include stent geometry as well as anatomical eye variations (i.e. sclera thickness etc.).

## References

- [1] Ethier, C.R., Johnson, M., Ruberti, J., 2004, "Ocular Biomechanics and Biotransport", Annual Review Biomedical Engineering, 6: 249-73.
- [2] Power, E. D., 2001, "A Nonlinear Finite Element Model of the Human Eye to Investigate Ocular Injuries From Night Vision Goggles". Thesis. Virginia Polytechnic Institute and State University, Blacksburg, Virginia
- [3] Rossi, T., Boccassini, B., Esposito, L., Iossa, M., Ruggiero, A., Tamburelli, C., Bonora, N., 2011, "The Pathogenesis of Retinal Damage in Blunt Eye Trauma: Finite Element Modeling", Investigative Ophthalmology and Visual Science June 7, 2011 vol. 52 no. 7: 3994-4002.
- [4] Chen, K., Rowley, A. P., Weiland, J. D., 2009, "Elastic Properties of Porcine Ocular Posterior Soft Tissues", Journal of Biomedical Materials Research Part A: 635-645.
- [5] Murgatroyd, H., Bembridge, J., 2008 "Intraocular Pressure", Continuing Education in Anesthesia, Critical Care and Pain, Vol. 8, Nr. 3: 100-103. s
- [6] Gray W., Sponse, E., Scribbeck, F.W., Stern, A.R., Weiss, C.E., Groth, S., Walker, J.D., "Numerical Modeling of Paintball Impact Ocular Trauma: Identification of Progressive Injury Mechanisms", IOVS, September 2011, Vol.52, No. 10.
- [7] Belaidi, A., and Pierscionek B. K., 2007, "Modeling Internal Stress Distributions in the Human Lens: Can Opponent Theories Coexist?" Journal of Vision 1st ser. 7.11: 1-12.
- [8] Chugh, D., 2012. "Finite Element Study of Nerve Fibers around Retinal Arteries and Possible Arteries and

- Possible Risk Factors for Glaucoma". Thesis. University of Florida.
- [9] Schachar, R. A., Abolmaali, A., 2006 "Proper Material Properties Are Required for the Finite Element Method." *Archives Ophthalmology* Vol. 124.
- [10] Le, T., 2005, "Nonlinear Finite Element Model Analysis of Human Accommodation Lens". Thesis. THE UNIVERSITY OF TEXAS AT ARLINGTON.
- [11] Wallensak G., Spoerl E, 2004 "Biomechanical Characteristics of Retina", *Retina*: Vol. 24,6 : 967-970.
- [12] Abolmaali, A., Schachar, R. A., and Le, T., 2007, "Sensitivity Study of Human Crystalline Lens Accommodation." *Computer Methods and Programs in Biomedicine* 85.1 : 77-90.
- [13] Bendre, A. A., 2009, "Finite Element Analysis and Preliminary Experiments to Study the Effects of High Myopia in Macular Degeneration ". Mechanical Engineering Master' S Theses. Northeastern University, Paper 22. [Http://hdl.handle.net/2047/d20000047](http://hdl.handle.net/2047/d20000047)
- [14] Eilaghi, A., 2009, "Effects of Scleral Stiffness on Biomechanics of the Optic Nerve Head in Glaucoma." Thesis. Department of Mechanical and Industrial Engineering University of Toronto.
- [15] Neeley, W. L., Redenti, S., Klassen, H., Tao, S., Desai, T., Young, M. J., Langer, R., 2008 "A Microfabricated Scaffold for Retinal Progenitor Cell Grafting." *Biomaterials* 29.4 418-426.
- [16] Olesen, C.G., Tertinegg, I., Eilaghi, A., Brodland, A.W., Horst, C., Veldhuis, J.H., Flanagan, J.G., Ethier, C.R. 2007, "Measuring the Biaxial Stress-Strain Characteristics of Human Sclera", *Proceedings of the 2007 ASME Summer Bioengineering Conference*, Paper SCB2007-176531.
- [17] Weeber, H. A., Van Der Heijde, G. L., 2007 "Internal Deformation of the Human Crystalline Lens during Accommodation." *Acta Ophthalmologica Scandinavica*
- [18] Weeber, H. A., Eckert, G., Soergel, F., Meyer, C. H., Pechhold, W., Van Der Heijde, R. G.L., 2005 "Dynamic Mechanical Properties of Human Lenses." *Experimental Eye Research* 80: 425-34
- [19] Wilde, G. S., 2011 "Measurement of Human Lens Stiffness for Modelling Presbyopia Treatments." Thesis. Brasenose College/ University of Oxford, 2011.
- [20] Fort Wayne Metals, 2013, "Medical Grade Nitinol Wire." [Http://www.fwmetals.com/](http://www.fwmetals.com/). Fort Wayne Metals, Web. 21 June 2013.